Improved Utilization of Nitrate Nitrogen Through Within-Leaf Nitrogen Allocation Trade-Offs in *Leymus chinensis*

Xiaowei Wei[1,2], Yuheng Yang[1], Jialiang Yao[1], Jiayu Han[1], Ming Yan[1], Jinwei Zhang[1], Yujie Shi[1], Junfeng Wang[1]* and Chunsheng Mu[1]*

[1] Key Laboratory of Vegetation Ecology of the Ministry of Education, Jilin Songnen Grassland Ecosystem National Observation and Research Station, Institute of Grassland Science, Northeast Normal University, Changchun, China, [2] Key Laboratory for Plant Resources Science and Green Production, Jilin Normal University, Siping, China

The Sharply increasing atmospheric nitrogen (N) deposition may substantially impact the N availability and photosynthetic capacity of terrestrial plants. Determining the trade-off relationship between within-leaf N sources and allocation is therefore critical for understanding the photosynthetic response to nitrogen deposition in grassland ecosystems. We conducted field experiments to examine the effects of inorganic nitrogen addition (sole NH_4^+, sole NO_3^- and mixed NH_4^+/NO_3^-: 50%/50%) on N assimilation and allocation by *Leymus chinensis*. The leaf N allocated to the photosynthetic apparatus (N_{PSN}) and chlorophyll content per unit area (Chl_{area}) were significantly positively correlated with the photosynthetic N-use efficiency (PNUE). The sole NO_3^- treatment significantly increased the plant leaf PNUE and biomass by increasing the photosynthetic N allocation and Chl_{area}. Under the NO_3 treatment, *L. chinensis* plants devoted more N to their bioenergetics and light-harvesting systems to increase electron transfer. Plants reduced the cell wall N allocation or increased their soluble protein concentrations to balance growth and defense under the NO_3 treatment. In the sole NH_4^+ treatment, however, plants decreased their N allocation to photosynthetic components, but increased their N allocation to the cell wall and elsewhere. Our findings demonstrated that within-leaf N allocation optimization is a key adaptive mechanism by which plants maximize their PNUE and biomass under predicted future global changes.

Keywords: leaf N allocation, nitrate, ammonium, photosynthetic nitrogen-use efficiency, cell wall, *Leymus chinensis*

INTRODUCTION

Nitrogen (N) plays a vital role in ecosystems. This mineral element is required for plant growth and is typically absorbed as ammonium (NH_4^+) or nitrate (NO_3^-). Ammonium N (NH_4^+), and nitrate (NO_3^-) are also the main forms of N loading associated with atmospheric deposition (Galloway et al., 2008; Stevens, 2019; Liang et al., 2020). The N-use strategies of plant species of different

functional types vary, and different plants thus respond differently to N additions (Xia and Wan, 2008) as the grasses acquire N from the soil and adopt more flexible strategies for different soil N sources to meet their high N demand (Callow, 1999). Generally, larger plant growth responses to NH_4^+-N than NO_3^--N addition have been found in terrestrial plants, but not in shrubs or grasses (Yan et al., 2019; Liang et al., 2020). However, the differences in the N form uptaken by different species (Marschner and Marschner, 2012; Grassein et al., 2015) are likely to reflect differences in the N uptake and N use efficiency of the species (Lu et al., 2021). The availability of co-provisional NO_3^- affects the accumulation and assimilation of NH_4^+ in roots and leaves (Prinsi and Espen, 2018). Uptake of NH_4^+ and NO_3^- is mediated by low and high affinity systems in higher plants (Haynes and Goh, 1978; Forde, 2000; Howitt and Udvardi, 2000). The uptake and utilization of NH_4^+-N and NO_3^--N by plants is critical for agricultural production and ecosystem stability (Tho et al., 2017; Luo et al., 2021).

The metabolism of carbon and N are interactively coupled across scales, from the leaf scale to the whole plant scale. Thus, changes in the availability of N at one of these scales are likely to affect the metabolic system at other scales (Liang et al., 2020). The assimilation NH_4^+ and NO_3^- affects several biochemical and molecular mechanisms, thus altering various specific physiological processes throughout the plant development process (Liu and von Wirén, 2017). The majority of species are sensitive to excess NH_4^+ because less energy is required to uptake this form, but at high concentrations, this molecule might trigger numerous metabolic disorders (Britto and Kronzucker, 2002; Hessini et al., 2013). Generally, plants exposed to excess NH_4^+ and NO_3^- display reduced growth, increased N metabolism-related enzymes, and modified photosynthetic physiological characteristics (Guo et al., 2008; Mu and Chen, 2021). Nitrate reductase (NR), nitrite reductase (NiR), Glutamine synthetase (GS) I, and GSII activities and the transcriptional levels of the corresponding genes in wheat seedlings are significantly reduced by N deficiency (Balotf et al., 2016). In general, the activity of N metabolism enzymes is significantly related to the synthesis of photosynthesis (Marschner and Marschner, 2012). The results of a meta-analysis showed that the effects of N deposition on 14 photosynthesis-related traits and affecting moderators and the associated plant trait responses depended on biological, experimental, and environmental moderators (Liang et al., 2020). Moderators that affect the responses of photosynthetic N metabolism have less been simultaneously considered in previous studies.

N is absorbed by plants and distributed in plant leaves in different forms, such as soluble components (e.g., nitrates, amino acids, and proteins) and insoluble components (e.g., cell walls, membranes, and other structures; Feng et al., 2009; Liu et al., 2018). Approximately half of the total leaf N is used for photosynthesis and is allocated to three main systems: the carboxylation, bioenergetics, and light harvesting systems (Hikosaka and Terashima, 1995; Takashima et al., 2004). Small changes in photosynthetic N can affect the carboxylation efficiency and photosynthetic N use efficiency (PNUE) of plants (Feng et al., 2009; Onoda et al., 2017). Cell walls are a major N sink in leaves and are used for plant defense (Evans and Poorter, 2001; Feng et al., 2009). Mass and thickness of cell wall changed in response to sink–source perturbation, which caused decreases in gm and photosynthesis in soybean and French bean (Sugiura et al., 2020). Many studies have focused on the leaf N allocation trade-offs among different leaf components (Takashima et al., 2004; Feng et al., 2009; Onoda et al., 2017). For example, invasive species allocate more leaf N to their carboxylation and bioenergetics systems than native species, leading to invasive plants having higher A_n, PNUE, and respiration efficiencies (Feng, 2008; Feng et al., 2009). The invasive species generally had lower LMA than natives, allocate more N to soluble protein, amino acids, and nucleic acids and less N to cell wall protein, aligning them closer to the "high-return" end of the leaf economics spectrum (Funk et al., 2013). Maize plants tend to invest relatively more N into bioenergetics to sustain electron transport under low-N-stress conditions (Mu et al., 2016). This suggests that plants were able to optimally allocate their nutrients to achieve an adaptive "functional balance." Storage N is used for coordinating leaf expansion and photosynthetic capacity in winter oilseed rape (*Brassica napus* L.) from emergence to senescence, thereby promoting leaf growth and biomass (Liu et al., 2018). The mechanisms by which NH_4^+-N and NO_3^--N are allocated and utilized in the photosynthetic carbon assimilation process have rarely been studied.

Grasslands play an important role in coping with global change (Liu et al., 2019; Shi et al., 2021). *Leymus chinensis* is a perennial rhizomatous grass that is often considered the foundational and dominant species in the eastern Eurasian steppe regions (Zhu, 2004). Additionally, in these regions, the N availability in the soils is often limited. Although N preferences have been studied in relatively few grassland species, these responses of grassland plants to N availability and relative preferences for NH_4^+ and NO_3^- are important in structuring natural grassland communities (Cui et al., 2017), but have also become of recent interest in managed grasslands. Adding a small amount of NH_4^+-N to NO_3^--N can significantly affect the photosynthesis, growth, and biomass accumulation of *L. chinensis* (Zhang et al., 2018). In addition, other studies have shown that NH_4^+-N is more suitable for *L. chinensis* growth than NO_3^--N or glycine (Li et al., 2018). The results of previous studies on the effects of NH_4^+-N to NO_3^--N on the growth and biomass accumulation of *L. chinensis* have extensively varied.

This study aimed to clarify the trade-offs of within-leaf N allocation to the upregulation of photosynthesis responding to the varying N supply conditions. To date, studies on the effects of N forms have mainly focused on plant preference and root growth (Gansel et al., 2001; Leghari et al., 2016; Cui et al., 2017; Kumar et al., 2020), whereas few have reported its effects on N assimilation and absorption and within-leaf N allocation. In the present study, the effects of different N forms (sole NH_4^+, sole NO_3^- and mixed NH_4^+/NO_3^-: 50%/50%) supply on leaf N assimilation and within-leaf N allocation were examined under field conditions to elucidate the physiological mechanism of NO_3^--N assimilation and leaf N allocation in

L. chinensis leaves, and to enrich the theory of N absorption in *L. chinensis* leaves.

MATERIALS AND METHODS

Plant Materials and Growth Conditions

The field experiment was carried out at the Jilin Songnen Grassland Ecosystem National Observation and Research Station in Jilin Province, Northeast Normal University, China (44°34'N, 123°31'E). The experimental site was located in the semi-arid, semi-humid, and temperate continental monsoonal climate zone. The study area was characterized by hot and rainy summers and cold and dry winters. The soil properties in 0–20 cm soil layer were as follows: pH 8.75; EC, 79.16 μs cm^{-1}; total N, 1.04 g kg^{-1}; total phosphorous (P); 68 g kg^{-1}; organic Carbon (C), 6.43 g kg^{-1}; NH_4^+-N 1.24 mg kg^{-1}; NO_3^--N 1.91 mg kg^{-1}. The mean temperature ranges from 4.6 to 6.5°C. The annual mean precipitation ranges from 280 to 620 mm, with the majority of rainfall falling between June and September, and the mean annual rainfall ranging from 1,200 to 1,300 mm (Guo et al., 2020; Shi et al., 2021). The pot experiment was conducted according to a complete randomized block design with six replicates, with the plastic pots (15 cm in diameter and 25 cm in depth) filled with chestnut soil (3.5 kg soil pot $^{-1}$).

Leymus chinensis (Trin.) Tzvel. (C_3 perennial rhizomatous grass) was widely distributed in northern China, eastern Mongolia, Transbaikalia, and Russia. It has good ecological adaptability and tolerance to drought, saline-alkali, and low temperature environment. Thus, it often forms *L. chinensis* steppes and meadows as a dominant species (Liu et al., 2019). On April 20, shoots of *L. chinensis* were transplanted into plastic pots, while shoots were collected from the eastern of Eurasia meadow steppe. Based on the investigation of the population density of natural *L. chinensis* grassland in the field experimental site during the green period (April 10- May 10), all species were planted with four individuals per pot in monoculture, and the plots were harvested on August 20. Additional N was applied at four different treatment levels: unfertilized treatment (N0), sole NH_4^+-N [as $(NH_4)_2SO_4$] (NH$_4$), sole NO_3^--N [as $Ca(NO_3)_2$] (NO$_3$), and mixture of both NH_4^+-N and NO_3^--N in ratio of 1:1 (NH$_4$NO$_3$) for a total of 10 g N m^{-2}. Two equal portions of each mixture was added into each pot (May 10 and June 6). In the previous research conducted in the north grassland, N deposition at 10 g N m^{-2} y^{-1} was the maximum amount (Zhang et al., 2017). The medium containing NH_4^+ as the only N source was buffered with $CaCl_2$ (39.7 g m^{-2}). In addition, the nitrification inhibitor dicyandiamide (DCD, 98.0%) was added to the NH_4^+ (10 mg m^{-2} y^{-1}) and NH$_4$NO$_3$ treatment (5 mg m^{-2} y^{-1}) to inhibit nitrification of NH_4^+. Other fertilizers (P, K, S) and micronutrients (Zn, B, Mn, Mo, Cu, and Fe) were applied for all treatments to ensure that plant growth was not limited by nutrients other than N. The plots were kept free of weeds, insects, and diseases during the growth season, and all mesocosms were exposed to natural precipitation events and less irrigation to ensure normal plant growth. The plots were harvested on August 20 during the post fruiting vegetation growth stage.

Gas Exchange Measurements and Chlorophyll Fluorescence

From 24 to 30 July 2019, the leaf assimilation rate (A_n, μmol m^{-2} s^{-1}), stomatal conductance (g_s, mmol m^{-2} s^{-1}), and internal CO_2 (C_i, μmol mol^{-1}) were measured using a CIRAS-3 portable photosynthesis system (PP Systems, United States) equipped with a CO_2 concentration at 400 μmol mol^{-1} in the leaf chamber, at 500 μmol s^{-1} flow rate, and at 25°C. The photosynthetic photon flux density (PPFD) of the leaf chamber was set to 1,600 μmol m^{-2} s^{-1} (with 90% red light, 5% blue light, and 5% white light) and 65% relative humidity. For the rapid A/C_i response curve (Stinziano et al., 2017), the CO_2 partial pressure was changed from 50 to 1,200 μmol mol^{-1}. In each pot, the 2nd and 3rd leaf from the tip of the shoot were used for leaf gas exchange measurements and conducted between 8:00 a.m. and 16:00 a.m. (six replicates).

The maximum rate of Rubisco carboxylation (V_{cmax}, μmol m^{-2} s^{-1}) and maximum rate of electron transport (J_{max}, μmol m^{-2} s^{-1}) were calculated by the A/C_i curves data and fitted by using the models of von Caemmerer (2000) and Long and Bernacchi (2003). The details were calculated as follows:

$$V_{cmax} = \frac{(R_d + A_n)\left[C_i + K_C\left(1 + \frac{O}{K_0}\right)\right]}{(C_i - \Gamma^*)}$$

$$J_{max} = \frac{4(R_d + A_n)(C_i + 2\Gamma^*)}{(C_i - \Gamma^*)}$$

where R_d is the mitochondrial respiration rate in the light (μmol m^{-2} s^{-1}), K_c and K_o are Michaelis constants for carboxylation and oxygenation, O is the intercellular oxygen concentration close to 210 mmol mol^{-1}, and Γ^* is the CO_2 compensation point in the absence of respiration (μmol mol^{-1}), Additionally, K_c, K_o, and Γ^* calculated by the temperature dependence function from Bernacchi et al. (2001, 2003).

The chlorophyll fluorescence was obtained in order to analyze PSII quantum efficiency of plants by using an IMAGING PAM M-series (Walz, Effeltrich, Germany), and dark period of the samples was dark for 30 min before measurements. The maximum quantum yield of PSII (Fv/Fm), the effective quantum yield of PSII (φPSII), non-photochemical quenching coefficient (NPQ), and electron transport rate (ETR, μmol e^{-1} s^{-1} m^{-2}) were calculated according to Zhou et al. (2021).

Biochemical Measurements

After the determination of the chlorophyll fluorescence parameters, the leaf area was determined with a portable leaf area meter (AM350, ADC Bio Scientific Ltd., Herts, United Kingdom). Two leaves per plant were collected, immediately frozen in liquid N, and stored at -80°C for biochemical analysis. Two additional leaves were halted enzyme activity at 105°C for 30 min of leaves and dried to a constant weight at 65°C. Then biomass was measured and analyzed for total N content (N_m, mg g^{-1}) with an Elementar Vario EL Cube (Elementar, Langenselbold, Germany). A leaf mass per unit leaf area (LMA, g m^{-2}) and a leaf N content per unit leaf area (N_{area}, g m^{-2}) were calculated as $N_{area} = N_m \times$ LMA. Chlorophyll per leaf mass (Chl_m, mg g^{-1})

was quantified by 0.1 g leaf in the ethanol extract, and measured using a spectrophotometer (UVmini-1240, Shimadzu, Japan) at 645 nm and 663 nm (Wellburn, 1994). The chlorophyll content was calculated as follows:

$$Chl_a = 12.43 \times A663 - 2.62 \times A645$$

$$Chl_b = 22.62 \times A645 - 4.36 \times A663$$

$$Chl_m = Chl_a + Chl_b$$

Chlorophyll per leaf area (Chl_{area}) was calculated as $Chl_{area} = Chl_m \times LMA$.

To quantify nitrate N and ammonium N contents in leaves, 2.0 g of lyophilized samples were incubated with 10 ml distilled water, boiled for 1 h, and filtered to obtain the crude extract. Subsequently, the NO_3^- concentration was measured by the salicylic acid chromogenic method of Cataldo et al. (1975), while NH_4^+ concentration was determined by the phenol-hypochlorite method of Felker (1977). Free amino acid was measured by ninhydrin colorimetric method (Hwang and Ederer, 1975).

Different forms of N were measured according to Takashima et al. (2004) and Onoda et al. (2017) with some modifications. The leaves were powdered with liquid N and homogenized in 2 ml of Na-phosphate buffer (pH 7.5, 100 mmol L^{-1}), then washed in a centrifuge tube. This procedure was repeated three times. The homogenates were centrifuged at 12,000 g at 4°C for 10 min, and the supernatant was regarded as soluble protein. The pellet was washed with 1 ml of phosphate buffer containing 3% sodium dodecyl sulfate (SDS), followed by centrifugation (12,000 g, 5 min) after heating in 90°C water for 5 min. This procedure was repeated six times while the supernatants regarded as SDS-soluble protein were collected. The residue, regarded as cell wall protein, was washed with ethanol into the quantitative filter paper. The supernatant was precipitated with 10% trichloroacetic acid (TCA) by heating at 85°C for 5 min. The precipitate was filtered with quantitative filter paper and washed with ethanol. The three types of components of N on the quantitative filter paper were dried at 85°C, and then analyzed by the Elementar Vario EL Cube.

Nitrate reductase, NiR, GSI, and GSII of frozen leaves was determined by plant NR, NiR, GSI, and GSII activity *ELISA* kit (Shanghai Enzyme Biotechnology Co., Ltd., China) according to the manufacturer's instructions.

Calculation of N Allocation in the Photosynthetic Apparatus and Photosynthetic N-Use Efficiency

According to the LUNA model developed by Niinemets and Tenhunen (1997), Niinemets et al. (2011), leaf photosynthetic N is divided into three major parts: the fractions of the total leaf N allocated to carboxylation system (PN_C, g g^{-1}), electron transport components (PN_B, g g^{-1}), and light harvesting components (PN_L, g g^{-1}). The photosynthetic apparatus were calculated as follows:

$$PN_C = \frac{V_{c\ max}}{6.25 \times V_{cr} \times N_{area}}$$

$$PN_B = \frac{J_{max}}{8.06 \times J_{mc} \times N_{area}}$$

$$PN_L = \frac{C_C}{N_{area} \times C_B}$$

where 6.25 (g Rubisco g^{-1} N) was the coefficient of Rubisco conversion into N at 25°C (Douglas et al., 1984), V_{cr} was 20.78 (μmol CO_2 g^{-1} Rubisco s^{-1}) at 25°C (Niinemets and Tenhunen, 1997), 8.06 was the N conversion coefficient of cytochrome (Nolan and Smillie, 1977), J_{mc} was the maximum electron transport rate per unit cytochrome f s^{-1} (155.65 μmol e^{-1} μmol cytochrome f s^{-1}) at 25°C (Niinemets and Tenhunen, 1997; Niinemets et al., 2011), Cc was leaf chlorophyll content (mmol g^{-1}), and C_B was chlorophyll binding to light harvesting components (2.15 mmol g^{-1} N; Hikosaka and Terashima, 1995). The fractions of leaf N allocated to the thylakoid ($PN_{B\ +\ L}$, g g^{-1}) and the photosynthetic apparatus (PN_{PSN}, g g^{-1}) were the sum of PN_B and PN_L, and the sum of PN_C, PN_B, and PN_L, respectively. N content in carboxylation (N_C, g m^{-2}), bioenergetics (N_B, g m^{-2}), light-harvesting system (N_L, g m^{-2}), and all components of the photosynthetic apparatus (N_{PSN}, g m^{-2}) were calculated as the products of PN_C, PN_B, PN_L, and PN_{PSN} with N_{area}, respectively. The remaining leaf N was defined as other N. Photosynthetic N use efficiency (PNUE, μmol g N^{-2} s^{-1}) was calculated by A_n/N_{area} (Poorter and Evans, 1998).

Statistical Analysis

All data were examined for a normal distribution (Kolmogorov-Smirnov test) and homogeneity of variance (Levene's test) and conducted using R version 4.0.4 (R Core Team, 2020). Analyses were performed using the "Tukey's HSD" function from "agricolae" package and differences were considered significant at $p < 0.05$. A linear correlation was performed using "perason" function from the "ggpmisc" package. The biplot were plotted using the package "ggplot2."

RESULTS

Leaf Physiological and Morphological Traits

The effects of N0, NH_4, NO_3, and NH_4NO_3 on V_{cmax}, J_{max}, and g_s were significant ($p < 0.05$) (**Figure 1**). The V_{cmax}, J_{max}, and g_s values of the NO_3 treatment were significantly higher than those of the N0, NH_4, and NH4NO3 treatments ($p < 0.05$) (**Figures 1A–C**). The leaf mass per area (LMA) measured under the NH_4 treatment was significantly higher than under the N0 treatment, but no significant difference was found between NO_3 and NH_4NO_3 (**Figure 1D**). The N0, NH_4, NO_3, and NH_4NO_3 treatments had significant effects ($p < 0.05$) on N_{area}, Chl_{area}, A_n, and PNUE (**Figures 1E–H**). The N_{area} measured under the NO_3 treatment was significantly higher than that under the N0 and NH_4 treatments ($p < 0.05$), but no significant difference was found between the NO_3 and NH_4NO_3 treatments (**Figure 1E**). The Chl_{area}, A_n, PNUE, and total leaf biomass measured under the NO_3 treatment were significantly higher than those under the N0, NH_4, and NH_4NO_3 treatments ($p < 0.05$) (**Figures 1F–I**).
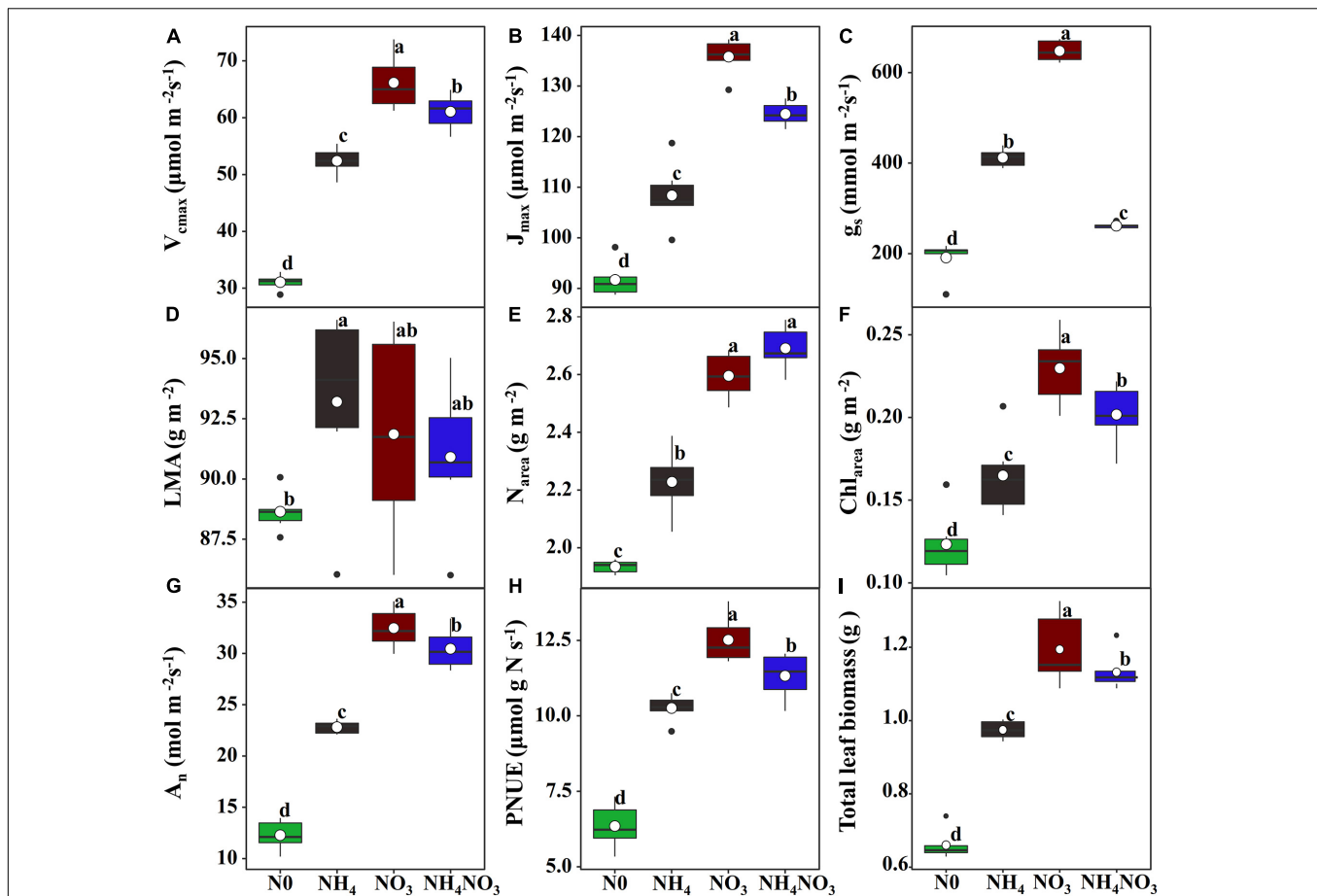
FIGURE 1 | Effect of N (N) forms treatments on maximum carboxylation rate (V_{cmax}) **(A)**, maximum photoelectron transfer rate (J_{max}) **(B)**, stomatal conductance (g_s) **(C)**, leaf mass area (LMA) **(D)**, area-based N content (N_{area}) **(E)**, area-based chlorophyll content (Chl_{area}) **(F)**, net CO_2 assimilation rate (A_n) **(G)**, photosynthetic N use efficiency (PNUE) **(H)**, and total leaf biomass **(I)** in *L. chinensis*. White dot is "Mean"; black dot is "Outlier"; horizontal is "Median"; the top of vertical line is "Max" and the bottom of vertical line is "Min." Different lower-case letters indicate significant differences between the measuring dates under the unfertilized (N0) treatment and the fertilized (NH_4, NO_3, NH_4NO_3) treatment, respectively ($p < 0.05$) ($n = 6$).

Leaf N Assimilation Enzyme Activity

To evaluate whether the induction of PNUE in the NH_4^+ and NO_3^- supply treatments was related to nitrate and ammonium accumulation or to the induction of NR, NiR, and GS activity, NR and NiR activities were stimulated in the NO_3 treatment. Conversely, they were inhibited in the NH_4 treatment (**Figures 2A,B**). In contrast, neither the GSI nor the GSII isoform activity was changed due to the effects of different N forms despite presenting higher values compared to the N0 treatment (**Figures 2C,D**).
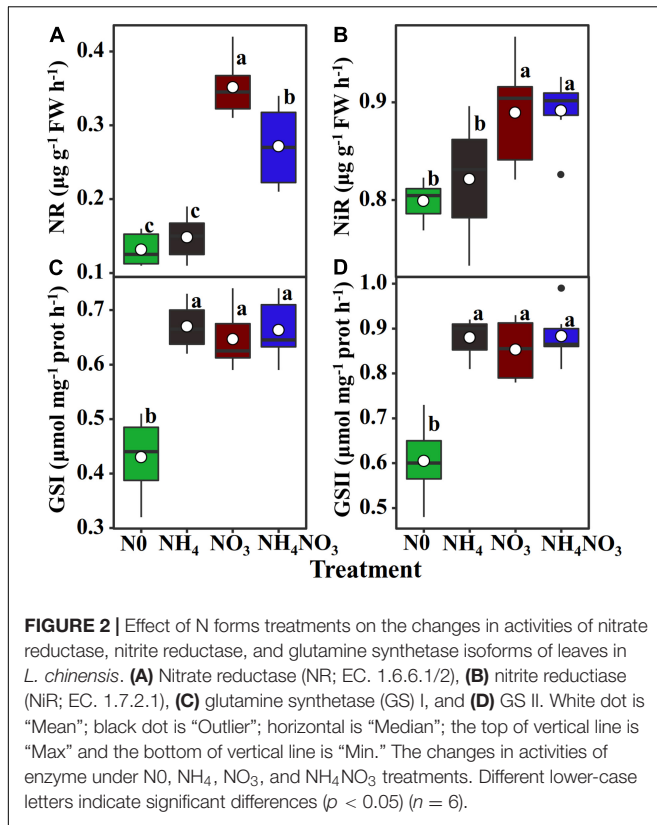
Leaf N Allocation to Other Soluble-N Components

The nitrate contents in the NO_3- and NH_4NO_3-treated plants were higher than those measured in plants under the N0 and NH_4 treatments ($p < 0.05$) (**Table 1**). However, in the NO_3 treatment, the leaf nitrate content was very low, accounting for approximately 0.87% of the total leaf N (**Figure 3C**). The ammonium content measured under the NH_4 treatment was

higher than those measured under the treatments with other N forms ($p < 0.05$) (**Table 1**), accounting for approximately 1.36% of the total leaf N (**Figure 3B**). Compared with the NH_4 treatment, the content of free amino acids was 21.07 and 31.44% higher under the NO_3 treatment and NH_4NO_3 treatment. The amount of N measured in other soluble protein was 10.88 and 19.62% higher under the NO_3 and NH_4NO_3 treatments than under the NH_4 treatment ($p < 0.05$) (**Table 1**).

Leaf N Allocation to Structure-N Components

The N_C (carboxylation) and N_B (bioenergetics) values expressed per unit leaf area were significantly higher under the NO_3 treatments than under the N0, NH_4, or NH_4NO_3 treatments ($p < 0.05$) (**Table 1** and **Figure 3**). No significant difference was found in N_L (light-harvesting system) between the NO_3 and NH_4NO_3 treatments, but N_L was significantly higher in these treatments than in the N0 and NH_4 treatments ($p < 0.05$) (**Table 1**). Compared to the N0, NH_4, and NH_4NO_3 treatments,

FIGURE 2 | Effect of N forms treatments on the changes in activities of nitrate reductase, nitrite reductase, and glutamine synthetase isoforms of leaves in *L. chinensis*. **(A)** Nitrate reductase (NR; EC. 1.6.6.1/2), **(B)** nitrite reductiase (NiR; EC. 1.7.2.1), **(C)** glutamine synthetase (GS) I, and **(D)** GS II. White dot is "Mean"; black dot is "Outlier"; horizontal is "Median"; the top of vertical line is "Max" and the bottom of vertical line is "Min." The changes in activities of enzyme under N0, NH_4, NO_3, and NH_4NO_3 treatments. Different lower-case letters indicate significant differences ($p < 0.05$) ($n = 6$).

$N_B/N_{B + L}$ decreased under the NO_3 and NH_4NO_3 treatments, while $N_L/N_{B + L}$ increased ($p < 0.05$) (**Figure 4B**). The leaf cell wall N content (N_{cw}) was 7.91% lower in the NO_3 treatment than in the NH_4 treatment (**Table 1**), while the cell wall per area was higher in the NH_4 treatment ($p < 0.05$) (**Figure 5**).

Within-Leaf N Allocation Estimate

The effects of different available N forms on the allocation of leaf N to different N components are shown in **Figure 3**.

Relative to the NH_4 and NH_4NO_3 treatments, the NO_3 treatment significantly increased the percentages of N allocated to carboxylation (1.31 and 1.75%, respectively), bioenergetics (0.24 and 0.36%), and light-harvesting system (3.7 and 1.5%) proteins. Unexpectedly, the amounts of N allocated to the nitrate and other soluble protein N components were elevated under NO_3 treatment. The percentage of N in free amino acid was 1.06 and 0.08% higher under NO_3 treatment than NH_4 and NH_4NO_3 treatments. Assessing the other N proportions, under the NO_3 treatment, the N proportions were 5.45, 1.54, and 1.38% lower than those measured under the N0, NH_4, and NH_4NO_3 treatments, respectively. The percentage of N allocated to cell walls exhibited a similar trend as the cell wall biomass under the different N forms. In summary, the correlation analyses revealed highly active relationships between N_{area} and PNUE and between N_{PSN} and PNUE (**Figures 6A,B**).

PSII Quantum Efficiencies

Since *L. chinensis* plants exhibited an advantage characterized by allocating N to photosynthetic components in leaves under the NO_3 treatment, we investigated whether nitrate and ammonium affect the PSII quantum efficiencies. Positive and highly significant linear relationships between PNUE and Chl_{area} were observed in *L. chinensis* (**Figure 6C**). The Fv/Fm, φPSII, non-photochemical quenching (NPQ), and electron transfer rate (ETR) were significantly higher under the NO_3 and NH_4NO_3 treatments than under the NH_4 and N0 treatments ($p < 0.05$) (**Figure 7**).
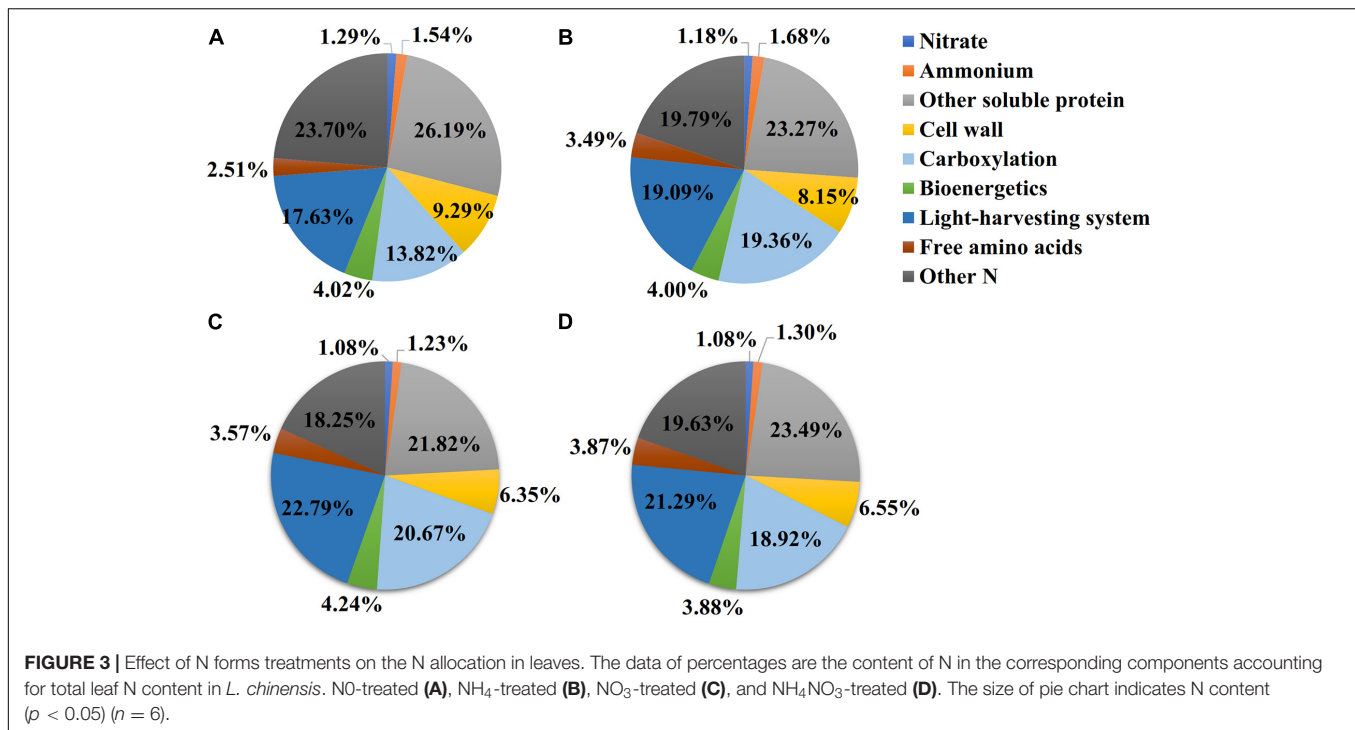
DISCUSSION

In this study, a set of experimental observations was conducted on the photosynthetic responses of *L. chinensis* (a C_3 plant) to varying N nutrient sources to capture leaf economics spectrum response mechanism. For a better understanding of absorption and utilization of nitrate N, observations ranged from plants' morphological features, trough overall photosynthesis, and

TABLE 1 | Effect of nitrotgen (N) forms treatments on the content of N compounds in *L. chinensis*.

Parameters (mg m^{-2})	N forms treatment			
	N0	NH$_4$	NO$_3$	NH$_4$NO$_3$
Nitrate	23.38 ± 0.33 c	25.53 ± 0.49 b	27.63 ± 0.38 a	27.72 ± 0.34 a
Ammonium	27.87 ± 0.66 c	36.27 ± 0.25 a	31.42 ± 0.81 b	33.30 ± 0.78 b
Free amino acids	45.40 ± 2.04 d	75.31 ± 2.24 c	91.18 ± 1.70 b	98.99 ± 1.43 a
Other soluble protein	473.66 ± 6.61 b	502.66 ± 17.76 b	557.35 ± 15.47 a	601.33 ± 27.29 a
Cell wall	168.04 ± 1.71 ab	175.96 ± 0.90 a	162.05 ± 3.93 b	167.56 ± 4.17 ab
Carboxylation	249.86 ± 4.21 d	418.06 ± 7.71 c	527.81 ± 15.87 a	484.15 ± 8.57 b
Bioenergetics	72.75 ± 1.01 d	86.37 ± 2.06 c	108.23 ± 1.18 a	99.22 ± 0.74 b
Light-harvesting system	318.74 ± 18.21 c	412.23 ± 25.64 b	582.08 ± 21.91a	544.80 ± 31.87a
Other N	428.26 ± 8.38b	427.35 ± 18.53 b	466.18 ± 14.57 ab	502.34 ± 26.67 a
Total N (g kg^{-1})	21.82 ± 0.05 d	23.90 ± 0.23 c	28.28 ± 0.29 b	29.60 ± 0.11 a

Data were reported as the arithmetic mean ± 1 standard error (n = 6). Numbers followed by different lower-case letters indicate significant differences, according to Tukey's test (p < 0.05).

FIGURE 3 | Effect of N forms treatments on the N allocation in leaves. The data of percentages are the content of N in the corresponding components accounting for total leaf N content in *L. chinensis*. N0-treated **(A)**, NH₄-treated **(B)**, NO₃-treated **(C)**, and NH₄NO₃-treated **(D)**. The size of pie chart indicates N content ($p < 0.05$) ($n = 6$).

within-leaf N allocation, up to photosynthetic component N and nutrient concentration in plants tissues. During the growing season, NH_4^+ and NO_3^- strongly affected each of investigated aspects of plant functioning and development.

As is well documented, N is an essential nutrient in plant growth and development, and its form can affect leaf growth (Cui et al., 2017). Leaf morphological adjustments are generally recognized to be more striking than leaf biochemical characteristics in determining leaf photosynthesis adaptations to the environment (Niinemets et al., 2011; Onoda et al., 2017). N promotes leaf area growth and helps leaves absorb light energy, thereby contributing to the maintenance of A_n and PNUE (Poorter and Evans, 1998; Onoda et al., 2017). The NO_3-treated plants showed higher g_s values than the plants exposed to other treatments. As expected, the increased g_s affected CO_2 assimilation and the higher V_{cmax} values suggest that biochemical restrictions should have also been reduced. According to Guo et al. (2003), nitrate is a well-known anionic transporter involved in the stomatal opening mechanism. This result also illustrates that the NO_3-treated plants had higher g_s values than the NH_4-treated plants. In the present study, *L. chinensis,* as a group, had no significant LMA with higher A_n, Chl_{area}, and N_{area} under NO_3 treatment compared to the N0, NH_4, and NH_4NO_3 treatments, resulting in the PNUE improving by 22.02 and 10.51%, respectively. In support of this idea, in *L. chinensis*, PNUE was positively correlated with N_{area}, N_{PSN}, and Chl_{area}. V_{cmax} is a proxy for the enzymatic activity of Rubisco during the photosynthetic carbon-fixation reactions (Farquhar et al., 1980; Sharkey, 2016; Zhuang et al., 2021). The inorganic N sources significantly increased the V_{cmax} and J_{max} of *L. chinensis*. Variations in V_{cmax} can be explained by changes in LMA, N_{area},

or the proportion of N allocated to the carboxylation system (Yin et al., 2019; Zhuang et al., 2021). These findings indicated that the NO3- supply is closely related to the normal growth of *L. chinensis* leaves.

Nitrate reductase and NiR participate in the process of reducing NO_3^- to NH_4^+ in coupled regulation (Kovács et al., 2015). In our study, the NO_3 treatment strongly stimulated the NR and NiR activities. This finding is consistent with previous studies reporting that NR activity is mainly affected by the concentration of NO_3^- (Balotf et al., 2016; Wen et al., 2019). When NO_3^- is converted to other forms of N, the availability of NO_3^- decreases, but the N in the soil was continuously transferred to the leaves, which led to an increase in the NO_3^- content and NR and NiR activities (Britto and Kronzucker, 2002; Marschner and Marschner, 2012). In higher plants, GSI and GSII assimilate NH_4^+ into amino acids for plant absorption and utilization in leaves (Bloom, 2015). Interestingly, although the concentration of NH_4^+ is closely related to GSI and GSII enzyme activities (Forde and Clarkson, 1999), GSI and GSII enzyme activities have no significant difference under N supply treatments, as has been previously reported for rice plants (Alencar et al., 2019; Sugiura et al., 2020). The results of this study reveal the relationships between the NO_3^- and NH_4^+ supply with assimilation enzyme activity. According to our results, the enzyme activity of N isozyme significantly increased under NO_3^- treatment.

Intra-leaf N allocation should reflect trade-offs in the economic spectrum of leaves, with faster-growing species allocating more N to metabolism at the expense of structure (Funk et al., 2013). Thus, we hypothesized that *L. chinensis* under NO_3- treatment, which are generally located on the
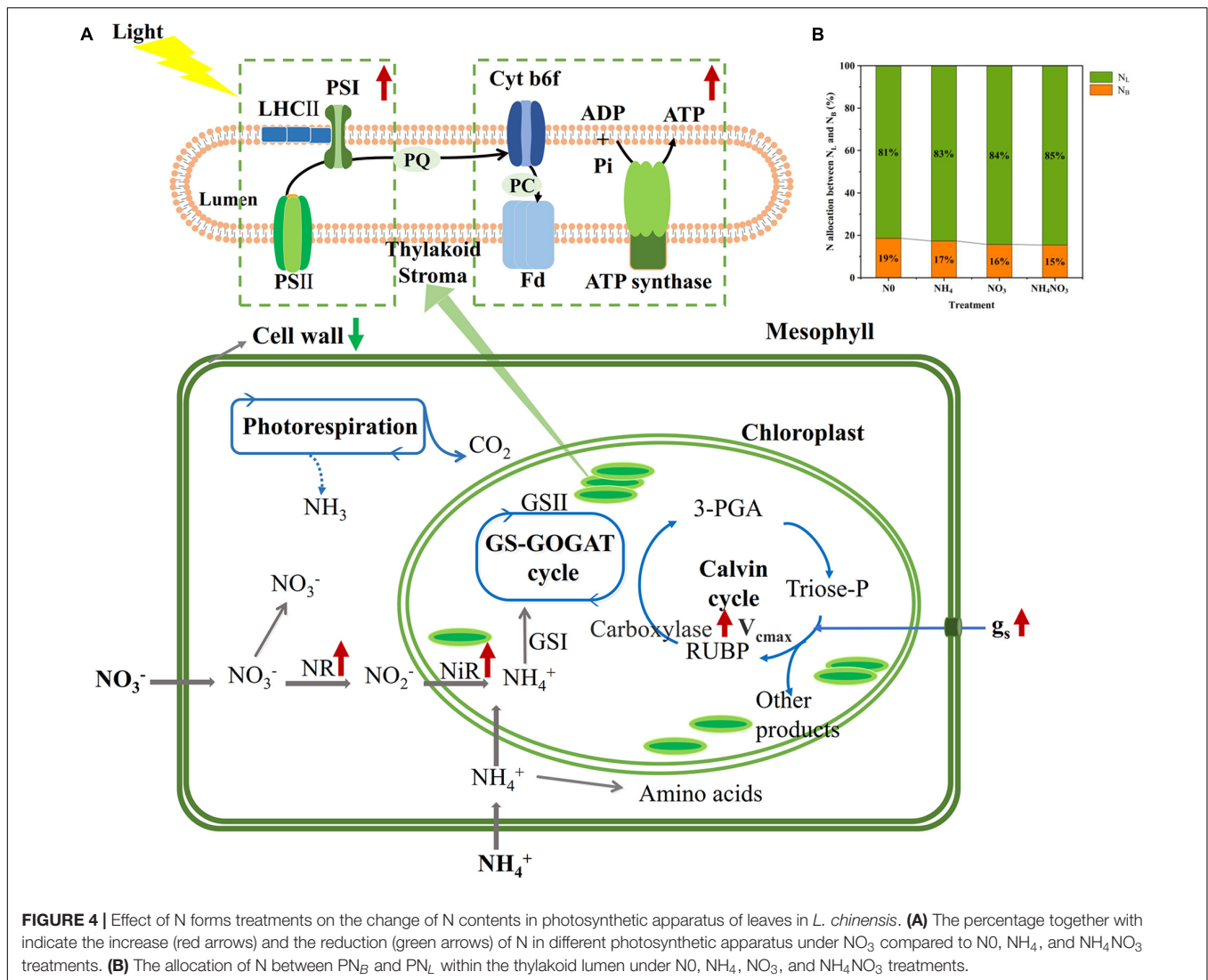
FIGURE 4 | Effect of N forms treatments on the change of N contents in photosynthetic apparatus of leaves in *L. chinensis*. **(A)** The percentage together with indicate the increase (red arrows) and the reduction (green arrows) of N in different photosynthetic apparatus under NO_3 compared to N0, NH_4, and NH_4NO_3 treatments. **(B)** The allocation of N between PN_B and PN_L within the thylakoid lumen under N0, NH_4, NO_3, and NH_4NO_3 treatments.

"high-return" of the leaf economics spectrum, would have higher A_n, N_{area}, and PNUE relative to other treatments. Therefore, it has greater allocation to leaf N pools associated with photosynthesis and growth. Species with greater N investments in photosynthetic proteins generally show higher PNUE in many natural ecosystems (Feng, 2008; Feng et al., 2009; Shi et al., 2019). Based on our original assumption of "high-return," we must assess the changes in the leaf N allocation process. In ecological models, N investments in the photosynthetic apparatus remain an important PNUE determinant (Feng et al., 2009; Liu et al., 2018). Photosynthesis is closely related to the leaf N content, which can be directly reflected by Calvin cycle proteins. Approximately three-quarters of leaf N is distributed to the photosynthetic apparatus (Dubreuil et al., 2017; Bahar et al., 2018; Zhang et al., 2020). In this study, *L. chinensis* allocated 47.7% of leaf N to the photosynthetic apparatus, and this was in accordance with previously reported results for rice plants (Zhong et al., 2019) and invade plants (Feng, 2008). Furthermore, we found that the amount of leaf N allocated to the

photosynthetic apparatus was significantly positively correlated with PNUE ($R^2 = 0.83$, $p < 0.001$). *L. chinensis* leaves have lower cell wall protein with higher amino acid content under NO_3-treated plants, consistent with allocation to growth at the expense of structure. However, our hypothesis that *L. chinensis* leaves would allocate more resources to carbon assimilation and growth at the expense of structure was only partially supported under NO_3-treated plants. *L. chinensis* also had higher amounts of total N and membrane-bound protein.

Nitrate treatment caused a relative increase in content of other soluble protein N and carboxylation N and the percentage (42.49%) of total soluble protein-N in total leaf N, similar to the result of Makino et al. (2003), who reported that 25–45% of leaf N was allocated to soluble proteins. Soluble proteins and free amino acids are two of the most abundant N sources, and they store N in leaves (Liu et al., 2018). Among soluble proteins, Rubisco is a key enzyme involved in C_3 photosynthesis (composing up to 50% of the leaf soluble protein and 25% of the leaf N; Lin et al., 2014). In the present study, the high photosynthetic N (N_{PSN}) and low
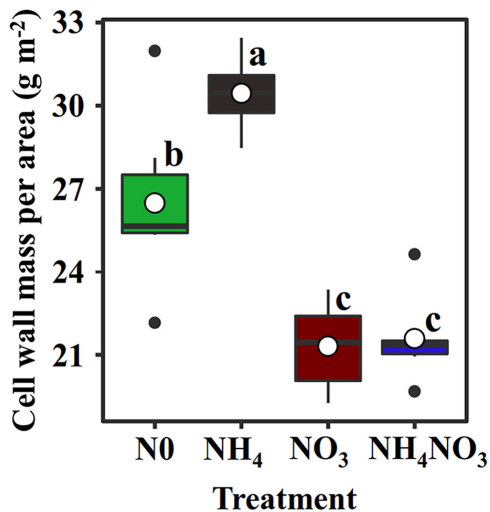
FIGURE 5 | Effect of N forms treatments on cell wall mass per area in *L. chinensis*. White dot is "Mean"; black dot is "Outlier"; horizontal is "Median"; the top of vertical line is "Max" and the bottom of vertical line is "Min." Different lower-case letters indicate significant differences under N0, NH_4, NO_3, and NH_4NO_3 treatments ($p < 0.05$) ($n = 6$).

cell wall N (N_{CW}) measured under the NO_3 treatment were presumably associated with a decrease in the cell wall biomass fraction (**Table 1** and **Figure 5**). Our finding that NO_3- treatment and other treatments have significant differences in the allocation of N to soluble protein, consistent with previously published results that faster grow species allocated more N to soluble protein at the expense of cell-wall protein (Feng et al., 2009; Landi and Esposito, 2017). Previous studies have highlighted that cell walls are a part of the plant apoplast, which is also an important N sink that can defend plants against stress (Feng et al., 2009; Shang et al., 2019). These results suggest that the allocation of N to cell walls was decreased under NO_3 conditions,

thus possibly contributing to the increased absorption and utilization of N and the maintenance of photosynthesis in mesophyll cells to the greatest extent possible. The N investment strategy regarding these N components was changed under NO_3 conditions, suggesting that these components are essential for ensuring adaptations of normal growth and physiological activities to inorganic N.

The NO_3^--N used in our field experiment resulted in relatively even allocation of N to photosynthetic apparatus (e.g., carboxylation, bioenergetics, and light-harvesting components) and carbon assimilation (e.g., soluble protein, free amino acids) functions. Our data matched the theoretical estimates modeled from photosynthetic data, indicating that C_3 plants invest about 24% leaf N to thylakoids and allocate 75% of thylakoids N to light harvesting proteins and 25% in bioenergetics (Poorter and Evans, 1998; Makino et al., 2003; Zhong et al., 2019; Mu and Chen, 2021). There are two types of thylakoid N, namely, one related to the bioenergetics system, such as the electron transport chain and photosynthetic phosphorylation, and another involved in the light-harvesting component (Mu et al., 2016). The absolute N content was devoted to biogenetics and light harvesting under the NO_3 treatment. Relatively more N from the thylakoid was allocated to bioenergetics under the different N treatments. *L. chinensis* leaves had higher A_n and V_{max} compared under NO_3-treated with other treatments. This suggests that Rubisco content or activity may have been higher in *L. chinensis* leaves. Our carboxylation fraction includes Rubisco, but Rubisco was not directly measured in this study. This proved that a leaf prioritization process occurred for the stabilization of the light harvesting and electron transfer systems under the NO_3 treatment and thus the maximization of the PSII quantum yield (Antal et al., 2010; Wang F. et al., 2019; Wang P. et al., 2019). This conclusion is supported by the finding that the Fv/Fm, φPSII, and ETR values were significantly different under the NO_3 treatment. Similarly, the higher NPQ measured under the NO_3 treatment should have helped dissipate excess electrons. The NO_3 treatment coincided with a higher leaf N concentration,
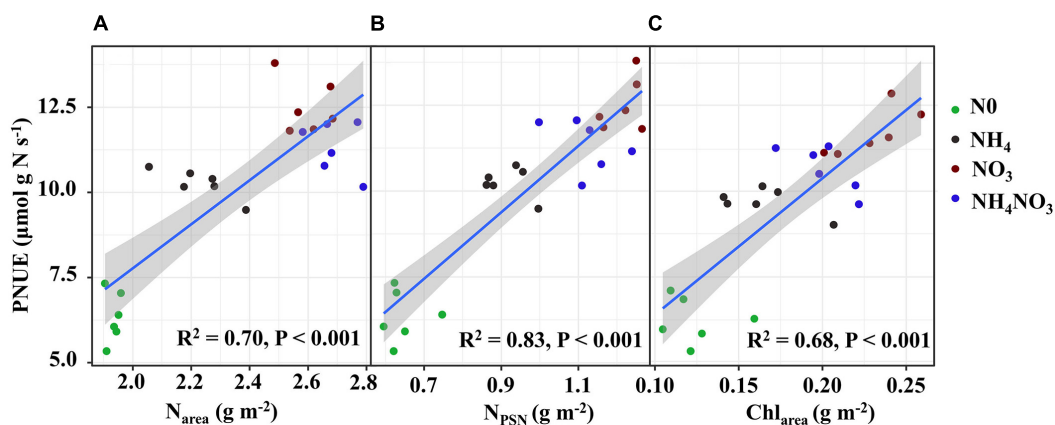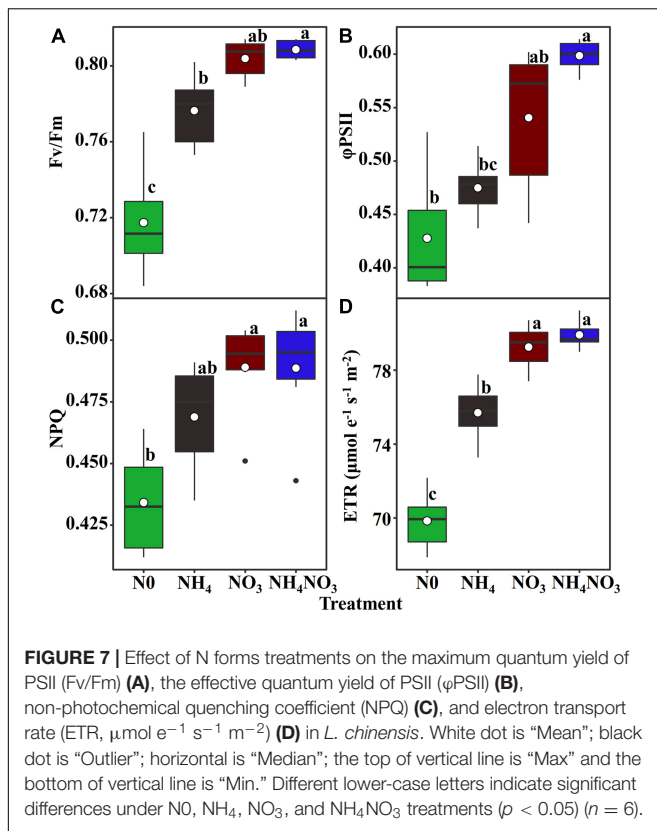

FIGURE 6 | Relationships of photosynthetic N use efficiency (PNUE) with area-based N content (N_{area}) **(A)**, photosynthetic N (N_{PSN}) **(B)** and area-based chlorophyll content (Chl_{area}) **(C)** in *L. chinensis*. The color of green, black, red, and blue correspond to the N0, NH_4, NO_3, and NH_4NO_3 treatments. Relationships between variables were assessed using linear regression analysis.

FIGURE 7 | Effect of N forms treatments on the maximum quantum yield of PSII (Fv/Fm) **(A)**, the effective quantum yield of PSII (φPSII) **(B)**, non-photochemical quenching coefficient (NPQ) **(C)**, and electron transport rate (ETR, μmol e^{-1} s^{-1} m^{-2}) **(D)** in *L. chinensis*. White dot is "Mean"; black dot is "Outlier"; horizontal is "Median"; the top of vertical line is "Max" and the bottom of vertical line is "Min." Different lower-case letters indicate significant differences under N0, NH$_4$, NO$_3$, and NH$_4$NO$_3$ treatments ($p < 0.05$) ($n = 6$).

and more N allocated to carboxylation compared to the other N treatments. It is likely that the relatively higher N in the bioenergetics and light-harvesting systems were well matched with the higher carboxylation capacity, promoting an increase in the photosynthetic rate and PNUE.

Our study examined within-leaf N partitioning in *L. chinensis* of the grassland dominant species in inorganic N absorption. *L. chinensis* leaves may succeed by allocating N to growth at the expense of higher leaf level carbon assimilation under NO$_3$$^-$ treatment. Furthermore, the leaf N assimilate enzyme activity and within-leaf N allocation were observed to exhibit different trends in response to the NO$_3$ treatment compared to the other treatments (**Figure 4**), suggesting that the trade-off between N assimilation and N allocation was specific and dependent on the prioritization of N forms for absorption in the plants. The proportion of the cell wall N allocation and other N to growth decreased under the NO$_3$ treatment. Under the NO$_3$ treatment, the proportions of N allocated to soluble proteins and the photosynthetic system increased, whereas the amount of N allocated to the cell wall was reduced, characterizing a trade-off between growth and defense in *L. chinensis*. In this vein, we analyzed whether NO$_3$$^-$ supply was able to induce PNUE improvement in leaves to establish if these changes could have contributed to promoted plant growth. The enzyme activity of N isozyme was significantly increased under NO$_3$$^-$ treatment. However, further accurate studies employing additional and more systematic approach are needed to definite the different NO$_3$$^-$ concentrations effected the leaf N allocation.

CONCLUSION

Our results evidence that NO$_3$$^-$ supply causes changes in some important photosynthetic processes in *L. chinensis* leaves. NO$_3$$^-$ induced increased in the NR and NiR enzyme activity which could have improved the process of reducing NO$_3$$^-$ to NH$_4$$^+$. N allocation was optimized within *L. chinensis* leaves, thus exhibiting an evolutional adaptation mechanism regarding the utilization of N for photosynthesis, thus increasing the PNUE and biomass during the growing season under NO$_3$ environment. Under the NO$_3$ treatment, *L. chinensis* plants tended to devote relatively more N to bioenergetics and the light-harvesting system to increase their ETR. Moreover, Chl$_{area}$ and NPQ were increased to reduce the damage caused by excess electron production. Within-leaf N allocation should reflect trade-offs in *L. chinensis* on the leaf economics spectrum with allocating more N to metabolic processes at the expense of structure. Taken together, the results of our study provide a comprehensive picture of the effects of nitrate N on within-leaf N assimilation and allocation and can help researchers obtain a better understanding of the mechanisms by which *L. chinensis* in meadow grasslands absorb and utilize NO$_3$$^-$-N under the context of increasing N deposition.

DATA AVAILABILITY STATEMENT

The original contributions presented in the study are included in the article/supplementary material, further inquiries can be directed to the corresponding author/s.

AUTHOR CONTRIBUTIONS

CM, JW, and XW designed the study. XW, MY, JH, and JY conducted the study. XW, YY, and JZ collected the data. XW and YS analyzed the data and wrote the manuscript. All authors read and approved the manuscript.

FUNDING

ACKNOWLEDGMENTS

REFERENCES

Alencar, V. T. C. B., Lobo, A. K. M., Carvalho, F. E. L., and Silveira, J. A. G. (2019). High ammonium supply impairs photosynthetic efficiency in rice exposed to excess light. *Photosynth. Res.* 140, 321–335. doi: 10.1007/s11120-019-00614-z

Antal, T., Mattila, H., Hakala-Yatkin, M., Tyystjärvi, T., and Tyystjärvi, E. (2010). Acclimation of photosynthesis to nitrogen deficiency in Phaseolus vulgaris. *Planta* 232, 887–898. doi: 10.1007/s00425-010-1227-5

Bahar, N. H. A., Hayes, L., Scafaro, A. P., Atkin, O. K., and Evans, J. R. (2018). Mesophyll conductance does not contribute to greater photosynthetic rate per unit nitrogen in temperate compared with tropical evergreen wet-forest tree leaves. *New Phytol.* 218, 492–505. doi: 10.1111/nph.15031

Balotf, S., Kavoosi, G., and Kholdebarin, B. (2016). Nitrate reductase, nitrite reductase, glutamine synthetase, and glutamate synthase expression and activity in response to different nitrogen sources in nitrogen-starved wheat seedlings. *Biotechnol. Appl. Biochem.* 63, 220–229. doi: 10.1002/bab.1362

Bernacchi, C. J., Pimentel, C., and Long, S. P. (2003). In vivo temperature response functions of parameters required to model RuBP-limited photosynthesis. *Plant Cell Environ.* 26, 1419–1430. doi: 10.1046/j.0016-8025.2003.01050.x

Bernacchi, C. J., Singsaas, E. L., Pimentel, C., Portis, A. R., and Long, S. P. (2001). Improved temperature response functions for models of Rubisco-limited photosynthesis. *Plant Cell Environ.* 24, 253–259. doi: 10.1111/j.1365-3040.2001.00668.x

Bloom, A. J. (2015). Photorespiration and nitrate assimilation: a major intersection between plant carbon and nitrogen. *Photosynth. Res.* 123, 117–128. doi: 10.1007/s11120-014-0056-y

Britto, D. T., and Kronzucker, H. J. (2002). NH4+ toxicity in higher plants: a critical review. *J. Plant Physiol.* 159, 567–584. doi: 10.1078/0176-1617-0774

Callow, J. A. (1999). *Advances in Botanical Research.* Cambridge: Academic Press.

Cataldo, D. A., Maroon, M., Schrader, L. E., and Youngs, V. L. (1975). Rapid colorimetric determination of nitrate in plant tissue by nitration of salicylic acid. *Commun. Soil Sci. Plant Anal.* 6, 71–80. doi: 10.1080/00103627509366547

Cui, J., Yu, C., Qiao, N., Xu, X., Tian, Y., and Ouyang, H. (2017). Plant preference for NH4+ versus NO3− at different growth stages in an alpine agroecosystem. *Field Crops Res.* 201, 192–199. doi: 10.1016/j.fcr.2016.11.009

Douglas, B., Jordan William, L., and Ogren. (1984). The CO2/O2 specificity of ribulose 1,5-bisphosphate carboxylase/oxygenase. *Planta* 161, 308–313. doi: 10.1007/BF00398720

Dubreuil, C., Jin, X., Barajas-Lopez, J. D., Hewitt, T. C., Tanz, S. K., Dobrenel, T., et al. (2017). Establishment of photosynthesis through chloroplast development is controlled by two distinct regulatory phases1. *Plant Physiol.* 176, 1199–1214. doi: 10.1104/pp.17.00435

Evans, J. R., and Poorter, H. (2001). Photosynthetic acclimation of plants to growth irradiance: the relative importance of specific leaf area and nitrogen partitioning in maximizing carbon gain. *Plant Cell Environ.* 24, 755–767. doi: 10.1046/j.1365-3040.2001.00724.x

Farquhar, G. D., Caemmerer, S., and von Berry, J. A. (1980). A biochemical model of photosynthetic CO2 assimilation in leaves of C3 species. *Planta* 149, 78–90. doi: 10.1007/BF00386231

Felker, P. (1977). Microdetermination of nitrogen in seed protein extracts with the salicylate-dichloroisocyanurate color reaction. *Anal. Chem.* 49:1080.

Feng, Y.-L. (2008). Nitrogen allocation and partitioning in invasive and native Eupatorium species. *Physiol. Plant* 132, 350–358. doi: 10.1111/j.1399-3054.2007.01019.x

Feng, Y.-L., Lei, Y.-B., Wang, R.-F., Callaway, R. M., Valiente-Banuet, A., Inderjit, et al. (2009). Evolutionary tradeoffs for nitrogen allocation to photosynthesis versus cell walls in an invasive plant. *Proc. Natl. Acad. Sci. USA* 106, 1853–1856. doi: 10.1073/pnas.0808434106

Forde, B. G. (2000). Nitrate transporters in plants: structure, function and regulation. *Biochim. Biophys. Acta* 1465, 219–235.

Forde, B. G., and Clarkson, D. T. (1999). "Nitrate and Ammonium Nutrition of Plants: Physiological and Molecular Perspectives," in *Advances in Botanical Research*, ed. J. A. Callow (Cambridge: Academic Press), 1–90. doi: 10.1016/j.plaphy.2020.06.051

Funk, J. L., Glenwinkel, L. A., and Sack, L. (2013). Differential allocation to photosynthetic and non-photosynthetic nitrogen fractions among native and invasive species. *PLoS One* 8:e64502. doi: 10.1371/journal.pone.0064502

Galloway, J. N., Townsend, A. R., Erisman, J. W., Bekunda, M., Cai, Z., Freney, J. R., et al. (2008). Transformation of the nitrogen cycle: recent trends, questions, and potential solutions. *Science* 320, 889–892. doi: 10.1126/science.1136674

Gansel, X., Muños, S., Tillard, P., and Gojon, A. (2001). Differential regulation of the NO3− and NH4+ transporter genes AtNrt2.1 and AtAmt1.1 in Arabidopsis: relation with long-distance and local controls by N status of the plant. *Plant J.* 26, 143–155. doi: 10.1046/j.1365-313x.2001.01016.x

Grassein, F., Lemauviel-Lavenant, S., Lavorel, S., Bahn, M., Bardgett, R. D., Desclos-Theveniau, M., et al. (2015). Relationships between functional traits and inorganic nitrogen acquisition among eight contrasting European grass species. *Ann. Bot.* 115, 107–115. doi: 10.1093/aob/mcu233

Guo, F.-Q., Young, J., and Crawford, N. M. (2003). The nitrate transporter AtNRT1.1 (CHL1) functions in stomatal opening and contributes to drought susceptibility in Arabidopsis. *Plant Cell* 15, 107–117. doi: 10.1105/tpc.006312

Guo, J., Li, H., Zhou, C., and Yang, Y. (2020). Effects of Flag Leaf and Number of Vegetative Ramets on Sexual Reproductive Performance in the Clonal Grass Leymus chinensis. *Front Plant Sci* 11:534278. doi: 10.3389/fpls.2020.534278

Guo, S., Zhou, Y., Li, Y., Gao, Y., and Shen, Q. (2008). Effects of different Nitrogen forms and osmotic stress on water use efficiency of rice (Oryza sativa). *Ann. Appl. Biol.* 153, 127–134. doi: 10.1111/j.1744-7348.2008.00244.x

Haynes, R. J., and Goh, K. M. (1978). Ammonium and nitrate nutrition of plants. *Biol. Rev.* 53, 465–510. doi: 10.1111/j.1469-185X.1978.tb00862.x

Hessini, K., Hamed, K. B., Gandour, M., Mejri, M., Abdelly, C., and Cruz, C. (2013). Ammonium nutrition in the halophyte Spartina alterniflora under salt stress: evidence for a priming effect of ammonium? *Plant Soil* 370, 163–173. doi: 10.1007/s11104-013-1616-1

Hikosaka, K., and Terashima, I. (1995). A model of the acclimation of photosynthesis in the leaves of C3 plants to sun and shade with respect to nitrogen use. *Plant Cell Environ.* 18, 605–618. doi: 10.1111/j.1365-3040.1995

Howitt, S. M., and Udvardi, M. K. (2000). Structure, function and regulation of ammonium transporters in plants. *Biochim. Biophys. Acta* 1465, 152–170. doi: 10.1016/S0005-2736(00)00136-X

Hwang, M. N., and Ederer, G. M. (1975). Rapid hippurate hydrolysis method for presumptive identification of group B streptococci. *J. Clin. Microbiol.* 1, 114–115. doi: 10.1128/jcm.1.1.114-115.1975

Kovács, B., Puskás-Preszner, A., Huzsvai, L., Lévai, L., and Bódi, E. (2015). Effect of molybdenum treatment on molybdenum concentration and nitrate reduction in maize seedlings. *Plant Physiol. Biochem.* 96, 38–44. doi: 10.1016/j.plaphy.2015.07.013

Kumar, V., Kim, S. H., Priatama, R. A., Jeong, J. H., Adnan, M. R., Saputra, B. A., et al. (2020). NH4+ suppresses NO3−-dependent lateral root growth and alters gene expression and gravity response in OsAMT1 RNAi mutants of rice (Oryza sativa). *J. Plant Biol.* 63, 391–407. doi: 10.1007/s12374-020-09263-5

Landi, S., and Esposito, S. (2017). Nitrate uptake affects cell wall synthesis and modeling. *Front. Plant Sci.* 8:1376. doi: 10.3389/fpls.2017.01376

Leghari, S. J., Wahocho, N. A., Laghari, G. M., HafeezLaghari, A., MustafaBhabhan, G., HussainTalpur, K., et al. (2016). Role of nitrogen for plant growth and development: a review. *Adv. Environ. Biol.* 10, 209–219.

Li, S., Jiang, F., Han, Y., Gao, P., Zhao, H., Wang, Y., et al. (2018). Comparison of nitrogen uptake in the roots and rhizomes of Leymus chinensis. *Biol. Plant.* 62, 149–156. doi: 10.1007/s10535-017-0748-1

Liang, X., Zhang, T., Lu, X., Ellsworth, D. S., BassiriRad, H., You, C., et al. (2020). Global response patterns of plant photosynthesis to nitrogen addition: a meta-analysis. *Glob. Change Biol.* 26, 3585–3600. doi: 10.1111/gcb.15071

Lin, M. T., Occhialini, A., Andralojc, P. J., Parry, M. A. J., and Hanson, M. R. (2014). A faster Rubisco with potential to increase photosynthesis in crops. *Nature* 513, 547–550. doi: 10.1038/nature13776

Liu, G., Li, X., and Zhang, Q. (2019). *Sheepgrass (Leymus chinensis): An Environmentally Friendly Native Grass for Animals.* Singapore: Springer.

Liu, T., Ren, T., White, P. J., Cong, R., and Lu, J. (2018). Storage nitrogen co-ordinates leaf expansion and photosynthetic capacity in winter oilseed rape. *J. Exp. Bot.* 69, 2995–3007. doi: 10.1093/jxb/ery134

Liu, Y., and von Wirén, N. (2017). Ammonium as a signal for physiological and morphological responses in plants. *J. Exp. Bot.* 68, 2581–2592.

Long, S. P., and Bernacchi, C. J. (2003). Gas exchange measurements, what can they tell us about the underlying limitations to photosynthesis? Procedures and sources of error. *J. Exp. Bot.* 54, 2393–2401. doi: 10.1093/jxb/erg262

Lu, P., Hao, T., Li, X., Wang, H., Zhai, X., Tian, Q., et al. (2021). Ambient nitrogen deposition drives plant-diversity decline by nitrogen accumulation in a closed grassland ecosystem. *J. Appl. Ecol.* 58, 1888–1898. doi: 10.1111/1365-2664.13858

Luo, X., Keenan, T. F., Chen, J. M., Croft, H., Colin Prentice, I., Smith, N. G., et al. (2021). Global variation in the fraction of leaf nitrogen allocated to photosynthesis. *Nat. Commun.* 12:4866. doi: 10.1038/s41467-021-25163-9

Makino, A., Sakuma, H., Sudo, E., and Mae, T. (2003). Differences between maize and rice in N-use efficiency for photosynthesis and protein allocation. *Plant Cell Physiol.* 44, 952–956. doi: 10.1093/pcp/pcg113

Marschner, H., and Marschner, P. (2012). *Marschner's mineral nutrition of higher plants*. London: Elsevier/Academic Press.

Mu, X., and Chen, Y. (2021). The physiological response of photosynthesis to nitrogen deficiency. *Plant Physiol. Biochem.* 158, 76–82. doi: 10.1016/j.plaphy.2020.11.019

Mu, X., Chen, Q., Chen, F., Yuan, L., and Mi, G. (2016). Within-leaf nitrogen allocation in adaptation to low nitrogen supply in maize during grain-filling stage. *Front. Plant Sci.* 7:699. doi: 10.3389/fpls.2016.00699

Niinemets, U., and Tenhunen, J. D. (1997). A model separating leaf structural and physiological effects on carbon gain along light gradients for the shade-tolerant species Acer saccharum. *Plant Cell Environ.* 20, 845–866. doi: 10.1046/j.1365-3040.1997.d01-133.x

Niinemets, U., Flexas, J., and Peñuelas, J. (2011). Evergreens favored by higher responsiveness to increased CO2. *Trends Ecol. Evol.* 26, 136–142.

Nolan, W. G., and Smillie, R. M. (1977). Temperature-induced changes in hill activity of chloroplasts isolated from chilling-sensitive and chilling-resistant plants. *Plant Physiol.* 59, 1141–1145. doi: 10.1104/pp.59.6.1141

Onoda, Y., Wright, I. J., Evans, J. R., Hikosaka, K., Kitajima, K., Niinemets, U., et al. (2017). Physiological and structural tradeoffs underlying the leaf economics spectrum. *New Phytol.* 214, 1447–1463. doi: 10.1111/nph.14496

Poorter, H., and Evans, J. R. (1998). Photosynthetic nitrogen-use efficiency of species that differ inherently in specific leaf area. *Oecologia* 116, 26–37. doi: 10.1007/s004420050560

Prinsi, B., and Espen, L. (2018). Time-course of metabolic and proteomic responses to different nitrate/ammonium availabilities in roots and leaves of maize. *Int. J. Mol. Sci.* 19:2202. doi: 10.3390/ijms19082202

R Core Team (2020). *R: A Language and Environment for Statistical Computing*. Vienna: R Foundation for Statistical Computing. Available online at: https://www.R-project.org/

Shang, B., Xu, Y., Dai, L., Yuan, X., and Feng, Z. (2019). Elevated ozone reduced leaf nitrogen allocation to photosynthesis in poplar. *Sci. Total Environ.* 657, 169–178. doi: 10.1016/j.scitotenv.2018.11.471

Sharkey, T. D. (2016). What gas exchange data can tell us about photosynthesis. *Plant Cell Environ.* 39, 1161–1163. doi: 10.1111/pce.12641

Shi, Y., Wang, J., Ao, Y., Han, J., Guo, Z., Liu, X., et al. (2021). Responses of soil N2O emissions and their abiotic and biotic drivers to altered rainfall regimes and co-occurring wet N deposition in a semi-arid grassland. *Glob. Chang. Biol.* 27, 4894–4908. doi: 10.1111/gcb.15792

Shi, Y., Wang, J., Le Roux, X., Mu, C., Ao, Y., Gao, S., et al. (2019). Trade-offs and synergies between seed yield, forage yield, and N-related disservices for a semi-arid perennial grassland under different nitrogen fertilization strategies. *Biol. Fertil. Soils* 55, 497–509. doi: 10.1007/s00374-019-01367-6

Stevens, C. J. (2019). Nitrogen in the environment. *Science* 363, 578–580. doi: 10.1126/science.aav8215

Stinziano, J. R., Morgan, P. B., Lynch, D. J., Saathoff, A. J., McDermitt, D. K., and Hanson, D. T. (2017). The rapid A-Ci response: photosynthesis in the phenomic era. *Plant Cell Environ.* 40, 1256–1262. doi: 10.1111/pce.12911

Sugiura, D., Terashima, I., and Evans, J. R. (2020). A decrease in mesophyll conductance by cell-wall thickening contributes to photosynthetic downregulation. *Plant Physiol.* 183, 1600–1611. doi: 10.1104/pp.20.00328

Takashima, T., Hikosaka, K., and Hirose, T. (2004). Photosynthesis or persistence: nitrogen allocation in leaves of evergreen and deciduous Quercus species. *Plant Cell Environ.* 27, 1047–1054. doi: 10.1111/j.1365-3040.2004.01209.x

Tho, B. T., Lambertini, C., Eller, F., Brix, H., and Sorrell, B. K. (2017). Ammonium and nitrate are both suitable inorganic nitrogen forms for the highly productive wetland grass *Arundo donax*, a candidate species for wetland paludiculture. *Ecol. Eng.* 105, 379–386. doi: 10.1016/j.ecoleng.2017.04.054

von Caemmerer, S. (2000). *Biochemical Models of Leaf Photosynthesis*. Clayton: CSIRO Publishing.

Wang, F., Gao, J., Shi, S., He, X., and Dai, T. (2019). Impaired electron transfer accounts for the photosynthesis inhibition in wheat seedlings (Triticum aestivum L.) subjected to ammonium stress. *Physiol. Plant* 167, 159–172. doi: 10.1111/ppl.12878

Wang, P., Wang, Z., Sun, X., Mu, X., Chen, H., Chen, F., et al. (2019). Interaction effect of nitrogen form and planting density on plant growth and nutrient uptake in maize seedlings. *J. Integrat. Agricult.* 18, 1120–1129. doi: 10.1016/S2095-3119(18)61977-X

Wellburn, A. R. (1994). The spectral determination of chlorophylls a and b, as well as total carotenoids, using various solvents with spectrophotometers of different resolution. *J. Plant Physiol.* 144, 307–313. doi: 10.1016/S0176-1617(11)81192-2

Wen, B., Li, C., Fu, X., Li, D., Li, L., Chen, X., et al. (2019). Effects of nitrate deficiency on nitrate assimilation and chlorophyll synthesis of detached apple leaves. *Plant Physiol. Biochem.* 142, 363–371. doi: 10.1016/j.plaphy.2019.07.007

Xia, J., and Wan, S. (2008). Global response patterns of terrestrial plant species to nitrogen addition. *New Phytol.* 179, 428–439. doi: 10.1111/j.1469-8137.2008.02488.x

Yan, L., Xu, X., and Xia, J. (2019). Different impacts of external ammonium and nitrate addition on plant growth in terrestrial ecosystems: a meta-analysis. *Sci. Total Environ.* 686, 1010–1018. doi: 10.1016/j.scitotenv.2019.05.448

Yin, L., Xu, H., Dong, S., Chu, J., Dai, X., and He, M. (2019). Optimised nitrogen allocation favours improvement in canopy photosynthetic nitrogen-use efficiency: Evidence from late-sown winter wheat. *Environ. Exp. Bot.* 159, 75–86. doi: 10.1016/j.envexpbot.2018.12.013

Zhang, J., Cun, Z., and Chen, J. (2020). Photosynthetic performance and photosynthesis-related gene expression coordinated in a shade-tolerant species Panax notoginseng under nitrogen regimes. *BMC Plant Biol.* 20:273. doi: 10.1186/s12870-020-02434-z

Zhang, L., Sun, Z., Xie, J., Wu, J., and Cheng, S. (2018). Nutrient removal, biomass accumulation and nitrogen-transformation functional gene response to different nitrogen forms in enhanced floating treatment wetlands. *Ecol. Eng.* 112, 21–25. doi: 10.1016/j.ecoleng.2017.12.021

Zhang, Y., Xu, W., Wen, Z., Wang, D., Hao, T., Tang, A., et al. (2017). Atmospheric deposition of inorganic nitrogen in a semi-arid grassland of Inner Mongolia, China. *J. Arid. Land* 9, 810–822. doi: 10.1007/s40333-017-0071-x

Zhong, C., Jian, S.-F., Huang, J., Jin, Q., and Cao, X. (2019). Trade-off of within-leaf nitrogen allocation between photosynthetic nitrogen-use efficiency and water deficit stress acclimation in rice (Oryza sativa L.). *Plant Physiol. Biochem.* 135, 41–50. doi: 10.1016/j.plaphy.2018.11.021

Zhou, X., Lyu, J., Sun, L., Dong, J., and Xu, H. (2021). Metabolic programming of Rhododendron chrysanthum leaves following exposure to UVB irradiation. *Funct. Plant Biol.* 48, 1175–1185. doi: 10.1071/FP20386

Zhu, T. C. (2004). *Biological and Ecological Study of Leymus Chinensis*. Changchun: Jilin Science and Technology Press.

Zhuang, J., Zhou, L., Wang, Y., and Chi, Y. (2021). Nitrogen allocation regulates the relationship between maximum carboxylation rate and chlorophyll content along the vertical gradient of subtropical forest canopy. *Agricult. Forest Meteorol.* 307:108512. doi: 10.1016/j.agrformet.2021.108512